Effects of Chemical Composition of $PM_{2.5}$ on Visibility in a Semi-rural City of Sichuan Basin

Yun-Chun Li[1,2+*], Man Shu[1+], Steven Sai Hang Ho[3**], Jian-Zhen Yu[4], Zi-Bing Yuan[4], Zi-Fang Liu[5], Xian-Xiang Wang[1], Xiao-Qing Zhao[1]

[1] *College of Science, Sichuan Agricultural University, Ya'an 625014, China*
[2] *Jiangsu Key Laboratory of Atmospheric Environment Monitoring and Pollution Control (AEMPC), School of Environmental Sciences and Engineering, Nanjing University of Information Science and Technology, Nanjing 210044, China*
[3] *Key Lab of Aerosol Chemistry & Physics, Institute of Earth Environment, Chinese academy of Sciences, Xi'an 710075, China*
[4] *Department of Chemistry, The Hong Kong University of Science and Technology, Clear Water Bay, Hong Kong, China*
[5] *Ya'an Environmental Monitoring Center, Ya'an 625014, China*

ABSTRACT

The rate of visibility deterioration in Ya'an city in the Sichuan Basin has been accelerating since the 2000s. Issues related to the air quality as well as meteorological conditions are reported in this study. Fine particulate matters ($PM_{2.5}$) were collected in Ya'an from June 2013 till June 2014. The chemical compositions of the samples were determined. The annual average visual range (VR), $PM_{2.5}$ concentrations, and ambient light extinction coefficient (b_{ext}) were 11.9 ± 9.2 km, 64.1 ± 41.6 µg m^{-3}, and 452 ± 314 Mm^{-1}, respectively. The highest concentration of $PM_{2.5}$, the highest b_{ext}, and the lowest VR were all seen in winter, followed by spring, autumn, and summer. Organic matter (OM), ammonium sulfate [$(NH_4)_2SO_4$], and ammonium nitrate [NH_4NO_3] were the major constituents, accounting for 32.8%, 28.3%, and 12.1%, respectively, of the total $PM_{2.5}$ mass. The revised Interagency Monitoring of Protected Visual Environments (IMPROVE) equation was applied to estimate ambient b_{ext}. On an annual basis, $(NH_4)_2SO_4$ was the most significant contributor (43.1%), followed by OM (27.1%) and NH_4NO_3 (22.4%), which, in total, accounted for 92.6% of the ambient b_{ext}. Rayleigh, elemental carbon, fine soil, nitrogen dioxide, and chloride salt accounted for a minor fraction (7.4%). Up to ~40.8% of the ambient b_{ext} was ascribed to relative humidity (RH), of which 26.4% and 14.0% were attributed to the hygroscopic growth of $(NH_4)_2SO_4$ and NH_4NO_3, respectively. More efforts are needed to reduce the average daily $PM_{2.5}$ concentration of < 59 µg m^{-3} to avoid the occurrence of haze under a high average RH of $78.3 \pm 10\%$, which significantly impacts visibility through various physico-chemical processes. Emissions of precursor gases, such as sulfur dioxide, nitrogen oxides, ammonia, and volatile organic compounds, should be reduced to improve the air quality and visibility in Ya'an.

Keywords: Fine particulate matter; Visibility; Light extinction coefficient; Chemical composition.

INTRODUCTION

Visibility, a fundamental metric of air quality, has been deteriorating globally from 1973 to 2007, especially occurred in southern and eastern Asia (Wang *et al.*, 2009). The trend is even more prominent in China, where has tremendous economic growth (Chang *et al.*, 2009; Wang *et al.*, 2013; Wu *et al.*, 2012; Zhang *et al.*, 2012). The decreases of atmospheric visibility, resulted in frequent haze, has become a major concern in China (Che *et al.*, 2009).

Visibility impairment is caused by the light scattering and absorption by atmospheric particles and gases. Light scattering is controlled by multiple factors, including concentration, size distribution, and chemical composition of ambient aerosols as well as meteorological conditions (Watson, 2002). Light extinction related to gaseous components in atmosphere are relatively well understood and estimated at various atmospheric conditions. For instance, the scattering by gases has been described with the Rayleigh scattering

---

[+] These authors contributed equally to this work.

[*] Corresponding author.
Tel.: +86-835-2886179; Fax: +86-835-2886139
E-mail address: yunchunli@sicau.edu.cn
[**] Corresponding author.
Tel.: +86-029-62336261
E-mail address: stevenho@hkpsrl.org

theory. In comparison, particle light extinction is more complex than that affected by gaseous components. Light-absorbing carbon such as soot and smoke from diesel exhaust or combustion processing and some crustal minerals are common airborne particle components that absorb lights. The amount of light scattered by an ensemble of particles can be accurately estimated using Mie theory when its size distribution and index of refraction are known. The scattering and absorption of the ensemble of particles can be calculated by summing up the optical and physical properties for each particle. However, it is rare that both intrinsic properties can be exactly measured in real environment. As a result, simplified calculation schemes are typically applied to make extinction estimates. An empirical formula, based on light extinction coefficient (b_{ext}) of the chemical species, was established by the Interagency Monitoring of Protected Visual Environments (IMPROVE) network and has been successfully used to estimate the relative contribution of components to the total light extinction (Pitchford *et al.*, 2007; Cao *et al.*, 2012; Li *et al.*, 2013; Wang *et al.*, 2015a). Fine particles ($PM_{2.5}$, particulate matter with an aerodynamic diameter less than 2.5 μm) lead visibility degradation due to their sizes similar as the wavelength of visible light, while the influences from gas and coarse particles on visibility degradation was relatively weak (Cheng and Tsai, 2000; Deng *et al.*, 2008; Wang *et al.*, 2012; Li *et al.*, 2013). Meteorological factors, including relative humidity (RH), wind, precipitation, temperature, have impacts on the concentration and optical property of $PM_{2.5}$ as well, thereby contributing to the visibility degradation (Malm *et al.*, 2003; Zhao *et al.*, 2011; Chen *et al.*, 2014).

Long-term trends of visibility, as well as the formation mechanism and particulate characteristics of low visibility events, have been investigated to identify pollution sources and determine effective air control strategies for developed Beijing-Tianjin-Hebei, Pearl River Delta, Yangtze River Delta regions in China (Deng *et al.*, 2008; Zhao *et al.*, 2011; Cheng *et al.*, 2013). Sulfate (SO_4^{2-}), nitrate (NO_3^-), ammonium (NH_4^+), and organic matter (OM) in $PM_{2.5}$ are the dominant contributors to light extinction and visibility impairment; secondary inorganic aerosols, coal combustion, biomass burning, engine exhaust, industry emission, fugitive dust are main sources of $PM_{2.5}$ and b_{ext} (Cao *et al.*, 2012; Li

et al., 2013; Wang *et al.*, 2013; Tao *et al.*, 2014). Compared with the developed regions, less attention has been drawn on the Sichuan basin, particularly its suburban and rural areas. However, the Sichuan basin, as known as "Envelope Basin" due to its envelope topography, has suffered from severe visibility degradation. In recent several decades, the highest aerosol optical depth among those Chinese cities was reported in Sichuan basin. It can be explained by high RHs and hygroscopic growth of aerosols due to water condensed on sulfate (Chen *et al.*, 2009; Henriksson *et al.*, 2011).

Urbanization and regional transport lead the suburban and rural areas in Sichuan basin to be polluted to some extent. However, there is still limited research conducted in the areas. Ya'an (102°51'–103°12'E, 29°40'–30°14'N) is a semi-rural city where located in the west margin of Sichuan basin. The city is 115 km away from Chengdu, the capital city of Sichuan Province, which is a transition zone not only between the Chengdu plain and the Qinghai-Tibetan plateau and also between urban centers and natural ecological areas. Fig. 1 indicates the special terrain of Sichuan basin and location of Ya'an. The city of Ya'an has an area of ~1.5 × 10^4 km² with a population of 1.53 million. The forest coverage rate is 51%. The region is known as "Rainy Area of West China" and "Rain city" with the average annual rainfall of 1,800 mm. Its climate can be characterized by high RHs, less sunshine, and low annual average temperature (14.1–17.9°C). To our best knowledge, only one report has demonstrated the visibility trends of Ya'an (Chen and Xie, 2012). Among those cities in Sichuan basin, Ya'an had the highest visibility and number of days with visibility > 19 km in the period of 1973 and 2010. However, a notable downward trend in 90th percentile visibility (i.e., a drop from 11.4 to 5.6 km) was shown and the number of low visibility (< 10 km) days increased at a rate of 16.2 days/decade. The objectives of this study are to characterize both of VR and b_{ext} in Ya'an, and to interpret the causes of visibility impairment by determining the relationship between b_{ext} and $PM_{2.5}$ and its chemical compositions.

METHODOLOGY

Site and Sampling

Sampling was conducted on the roof of a ten-storey
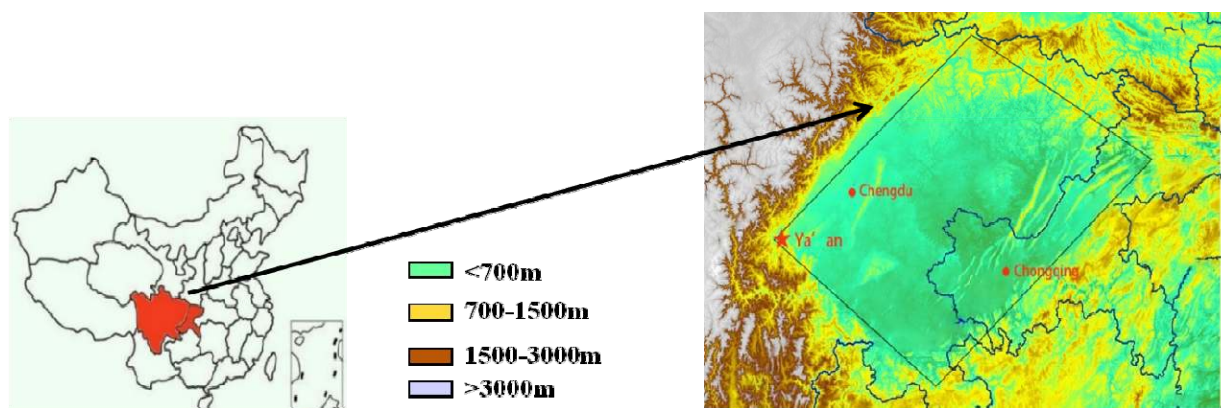

Fig. 1. A map of Sichuan basin and Ya'an city.

building on the campus of Sichuan Agricultural University in Ya'an from June 19, 2013 to June 26, 2014. No obvious pollution source was found nearby the semi-rural site. Twenty-four integrated $PM_{2.5}$ samples (from 10:00 to 10:00 the next day) were collected on pre-fired (at 500°C for 8 h) quartz-fiber filters (25×20 cm^2, Staplex, Brooklyn, New York, USA) every sixth of the day. A high-volume sampler (TE-6070-2.5, Tisch Environmental, Inc., Cleves, OH, USA) was operated at a flow rate of 1.13 m^3 min^{-1}. Due to the sampler fault, no sample was collected on Feb. 2 and Feb. 8, 2014. Rather than 61 routine samples, nine samples were collected at characteristic conditions, including at extremely high and low visibilities, on the Spring Festival, and within plowing season. A blank sample was collected for every season. All samples were wrapped with aluminum foil, and stored in a freezer at –18°C until chemical analysis to avoid evaporation of volatile compounds.

Chemical Analysis

Carbonaceous fractions (i.e., organic carbon [OC] and element carbon [EC]) were determined using a thermal/optical aerosol carbon analyzer (Sunset Laboratories, Forest Grove, OR, USA) with NIOSH method 5040 protocol (Birch and Cary, 1996). A filter punch of 1×1 cm^2 in size was removed from each filter and loaded into the aerosol carbon analyzer. Duplicate measurements of OC and EC were made on every ten sample, and the average relative standard deviations (RSD) were 4% and 9% for OC and EC, respectively (Yu *et al.*, 2002).

Water-soluble ions were measured using a Dionex ICS-3000 ion chromatography (IC, Sunnyvale, CA, USA). A punch of 4 cm^2 loaded filter was placed in centrifuge tube containing 10 mL of ultrapure water, that was then extracted in an ultrasonic bath for 1 h. The extract was filtered with 0.45 μm pore size microporous membrane, and the filtrate was stored at 4°C until analysis. Five cations (i.e., Na$^+$, NH$_4^+$, K$^+$, Mg^{2+} and Ca^{2+}) and five anions (i.e., MSA$^-$, C$_2$O$_4^{2-}$, Cl$^-$, NO$_3^-$ and SO$_4^{2-}$) were quantified. Details of analytical method were shown in previous study (Yang *et al.*, 2005).

Trace elements, including Mg, Al, Ca, Ti, V, Cr, Mn, Fe, Ni, Cu, Zn, As, Sr, Zr, Mo, Cd, Ba, Pb, were quantified by inductively coupled plasma-mass spectrometry (ICP-MS, Thermo Fisher, Finnigan, Germany) after microwave-assisted digestion (Swami *et al.*, 2001). A filter punch of 47 mm diameter was digested with an acid mixture of nitric acid (HNO$_3$):hydrogen peroxide (H$_2$O$_2$) (5:2, v/v) (Merck, Darmstadt, Germany) in a microwave digestion system (DuoPur, Milestone, Sorisole, Italy). Rhodium was added as an internal standard. Quality assurance and control of the ICP-MS was guaranteed by the analysis of a certified NIST urban particulates reference standard (SRM-1648). The recoveries of the target elements were in the range of 61%–92%, with SD < 10%.

The four field blanks were processed and analyzed as the same way as the samples. All sample results were corrected for the average of the blank levels. Replicate analysis (n = 7) were done for each group of ten samples. The RSD of the replicate analysis were < 5% and < 20% for the ion

species and trace elements, respectively. The correlation coefficients (R^2) of the calibrations were better than 0.99 (with a confidence level of 99.9%, n = 6) for all the chemical analyses.

Data Analysis
Reconstruction of $PM_{2.5}$ Mass

No $PM_{2.5}$ mass was measured by gravimetric method in this study due to only high-volume filter samples being collected. Source reconstruction techniques was thus applied to estimate its concentration with the equation of (Brook *et al.*, 1997):

$$[PM_{2.5}] = [SNA] + [OM] + [EC] + [FS] + [CS] + [TEO] + [K_{BB}] + [water] \tag{1}$$

where the concentration units of those chemical component are in μg m^{-3} (the same unit was applied in the texts thereafter). The major components considered in this study included secondary inorganic aerosols [i.e., SO$_4^{2-}$, NO$_3^-$, and NH$_4^+$, namely as SNA], OM, EC, fine soil (FS), chloride salt (CS), trace element oxide (TEO), biomass burning-derived K$^+$ (K$_{BB}$), and water. The thermodynamic equilibrium model-ISORROPIA II (reserve mode) (Fountoukis and Nenes, 2007) was applied to calculate the water contents at a fixed RH of 40% and temperature of 20°C.

SNA was in the forms of ammonium sulfate ((NH$_4$)$_2$SO$_4$), ammonium hydrogen sulfate (NH$_4$HSO$_4$) and ammonium nitrate (NH$_4$NO$_3$). If one assumes that the dominant compounds were NH$_4$HSO$_4$ and NH$_4$NO$_3$, the NH$_4^+$ concentration can be calculated using Eq. (2); alternatively if NH$_4^+$ were in the form of (NH$_4$)$_2$SO$_4$ and NH$_4$NO$_3$, then Eq. (3) would be applied:

$$[NH_4^+] = 0.29 \times [NO_3^-] + 0.19 \times [SO_4^{2-}] \tag{2}$$

$$[NH_4^+] = 0.29 \times [NO_3^-] + 0.38 \times [SO_4^{2-}] \tag{3}$$

where [NH$_4^+$], [NO$_3^-$], and [SO$_4^{2-}$] are the mass concentrations of NH$_4^+$, NO$_3^-$ and SO$_4^{2-}$, respectively. A comparison of the calculated and measured [NH$_4^+$] is presented in Fig. 2. The calculated [NH$_4^+$] from both Eq. (2) and Eq. (3) had strong correlations with the observed [NH$_4^+$], but the slope from Eq. (3) was closer to unity (1.04, refer to Fig. 2(a)) than that from Eq. (2) (0.69, Fig. 2(b)). If exclude the highest calculated data, the slope from Eq. (3) was almost equal to unity (1.01, n = 69). This indicates that the three ions predominantly existed as (NH$_4$)$_2$SO$_4$ and NH$_4$NO$_3$, and therefore the SNA concentration can be calculated by multiplying the SO$_4^{2-}$ and NO$_3^-$ concentrations by factors of 1.38 and 1.29, respectively.

Considering that relatively high OC/EC ratios (an average of 11) in this semi-rural city, OM is derived from multiplying OC concentrations by a factor of 1.8 to account for unmeasured atoms, such as hydrogen, oxygen, and nitrogen in OM (Turpin and Lim, 2001; Chen and Yu, 2007). The concentrations of FS are often estimated by assuming the oxides of the elements mainly associated with soil, which was described by Malm *et al.* (1994) as:
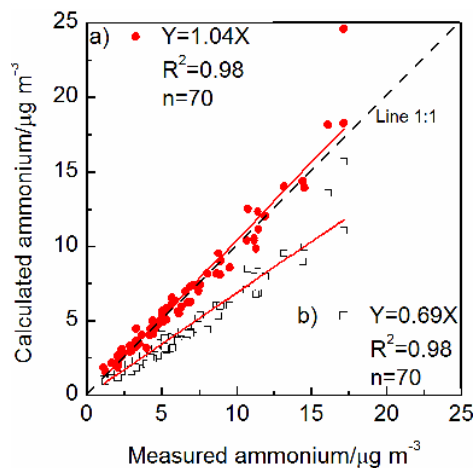
Fig. 2. Comparison of measured and calculated ammonium. Note: a) and b) are calculated by Eq. (3) and Eq. (2), respectively.
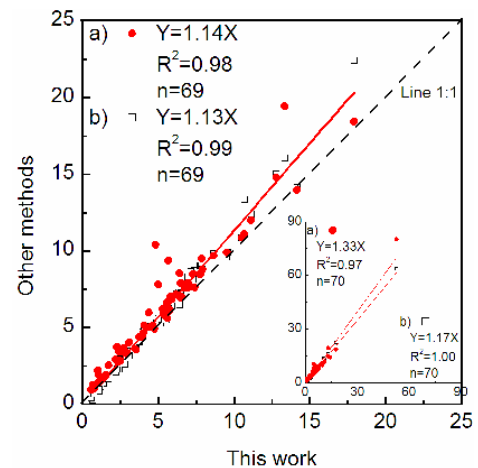

Fig. 3. Comparison of the estimated fine soil concentrations ($\mu g\ m^{-3}$) between Eq. (4) (this work) and a) Eq. (5) and b) Eq. (6), respectively.

$$[FS] = 2.20 \times [Al] + 2.49 \times [Si] + 1.63 \times [Ca] + 2.42 \times [Fe] + 1.94 \times [Ti] \quad (4)$$

However, silicon (Si) was not measured because quartz-fiber filters containing SiO_2 were used for sample collection in this study. We thus assumed the concentration of Si to be thrice that of aluminum (Al), which essentially agreed with measurement in soil dust collected in China demonstrated in a previous study (Bi *et al.*, 2007). There are two additional equations for calculations of FS concentrations using Eq. (5) (Brook *et al.*, 1997) and Eq. (6) (Hsu *et al.*, 2008):

$$[FS] = 2.20 \times [Al] + 2.49 \times [Si] + 1.63 \times [Ca] + 1.58 \times [Fe] + 1.94 \times [Ti] + 1.41 \times [K] \quad (5)$$

$$[FS] = 12.5 \times [Al] \quad (6)$$

Interestingly, the results obtained from the Eq. (4) and Eq. (6) were very consistent (Fig. 3), which had higher correlation ($R^2 = 1.00$, n = 70) than those from the Eq. (4) and Eq. (5) ($R^2 = 0.97$, n = 70), suggesting that potassium (K) in $PM_{2.5}$ was not mainly from soil in this study. It should be noted that the [FS] are hence reported using the Eq. (4).

The concentrations of sea salt was generally calculated as:

$$[\text{Sea salt}] = 2.54 \times [Na^+] \quad (\text{Ho } et\ al., 2003) \quad (7)$$

$$[\text{Sea salt}] = (1.82 \times [Cl^-] + 2.54 \times [Na^+])/2 \quad (8)$$

$$[\text{Sea salt}] = 1.82 \times [Cl^-] \quad (\text{Malm } et\ al., 1994) \quad (9)$$

Given that Sichuan basin is located inland, sea spray-generated sea salt particles are not readily transported and insignificantly contributed to its fine aerosols. We thus defined chloride salt, instead of sea salt, as the total concentration of Cl^-, Na^+, and Mg^{2+} (Eq. (10)),

$$[CS] = [Cl^-] + [Na^+] + [Mg^{2+}] \quad (10)$$

that had been successfully evaluated by Hsu *et al.* (2010a). In this study, the results derived by Eq. (7) and Eq. (9) are not consistent (refer to compare lines between (a) and (c) in Fig. 4). Furthermore, our results have a certain degree of over- or under-estimation when they were compared to those derived from these two methods (Fig. 4). However, the results derived from using our definition of chloride salt are very close to the average values calculated from the two methods (Eq. (8)), with a mean ratio of 0.94 and an excellent R^2 of 0.99 (n = 69, Fig. 4(b)). This supports the validity of our method, even though we realized that a portion of Cl^-, Na^+, and Mg^{2+} might originate from anthropogenic sources (in the case of Cl^-) and/or mineral soils (in the case of Na^+ and Mg^{2+}).

According to the methods shown in Landis *et al.* (2001) and Hsu *et al.* (2010), we estimated the contributions of heavy metals as TEO. Moreover, considering that additional trace metals which have been analyzed in our study, their
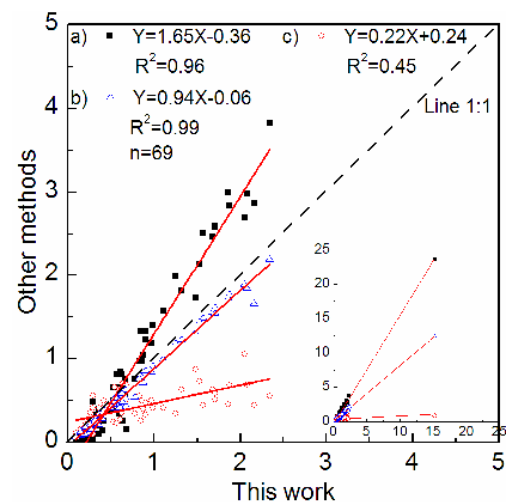

Fig. 4. Comparison of the estimated chloride salt concentrations ($\mu g\ m^{-3}$) between Eq. (10) (this work) and a) Eq. (7), b) Eq. (8), and c) Eq. (9), respectively.

enrichment factors (EFs) have been calculated as the equations:

$$TEO = 1.3 \times [0.5 \times (V + Ni + Sr + Ba) + 1 \times (Cr + Mn + Cu + Zn + As + Mo + Cd + Pb)] \tag{11}$$

$$EF_{crust} = (C_X/C_{Al})_{aerosol}/(C_X/C_{Al})_{crust} \tag{12}$$

where $(C_X/C_{Al})_{aerosol}$ is the concentration ratio of a given element X to Al in aerosols, and $(C_X/C_{Al})_{crust}$ is the concentration ratio of a given element X to Al in the average crustal abundance (Taylor, 1964). The degree to which the element X in an aerosol sample is enriched or depleted relative to a specific source (e.g., average crust) can be assessed using EF values. According to the EFs (shown in Table S1), all target trace elements were considered in different weights. An element which has an EF ≤ 1.0, such as Ti and Zr, was not taken into accounting, since it is identified to be of exclusive crustal origin. Elements having EFs between 1 and 10 were multiplied by a factor of 0.5, as they are identified as originated from both anthropogenic and crustal sources. For an element which has an EF ≥ 10, it was multiplied by unity as it is dominated from anthropogenic origins. Furthermore, the multiplicative factor was simply set to 1.3 for conversion of metal abundance to oxide abundance, while no adequate literature information on metal speciation was available for evaluation (Hsu *et al.*, 2010).

Reconstruction of the Light Extinction Coefficient

Atmospheric light extinction (b_{ext}) can be expressed as the sum of light scattering by particle (b_{sp}), absorption by particle (b_{ap}), scattering by gases (b_{sg}), and absorption by gases (b_{ag}). Reconstruction b_{ext} value is calculated based on the revised IMPROVE algorithm as follows (Pitchford *et al.*, 2007):

$$
\begin{aligned}
b_{ext} = {} & b_{sp} + b_{ap} + b_{sg} + b_{ag} \\
\approx {} & 2.2 \times f_S(RH) \times [\text{Small (NH}_4)_2\text{SO}_4] \\
& + 4.8 \times f_L(RH) \times [\text{Large (NH}_4)_2\text{SO}_4] \\
& + 2.4 \times f_S(RH) \times [\text{Small NH}_4\text{NO}_3] \\
& + 5.1 \times f_L(RH) \times [\text{Large NH}_4\text{NO}_3] \\
& + 2.8 \times [\text{Small OM}] + 5.1 \times [\text{Large OM}] \\
& + 10 \times [\text{EC}] + 1 \times [\text{FS}] + 1.7 \times f_{SS}(RH) \times [\text{Sea salt}] \\
& + 0.6 \times [\text{Coarse Mass}] + \text{Rayleigh Scattering} \\
& + 0.33 \times [\text{NO}_2 \, (\text{in ppb})]
\end{aligned}
\tag{13}
$$

where $0.33 \times [\text{NO}_2 \, (\text{in ppb})]$ presents absorption of gases (b_{ag}); Rayleigh scattering (b_{sg}) is 11 Mm^{-1} for all samples considering the elevation of sampling site is ~0.7 km; and the total of other 10 terms represent the sum of particle scattering and absorption (b_{sp} and b_{ap}), which estimated by multiplying the concentrations of each major components by typical component-specific mass extinction efficiencies. The $(NH_4)_2SO_4$, NH_4NO_3, and sea salt mass extinction efficiency terms include a water growth factor that is a function of RH (displayed as $f(RH)$) multiplying by a constant dry extinction efficiency. $f_S(RH)$ and $f_L(RH)$ are the water growth factors for small- and large-sized distribution of $(NH_4)_2SO_4$ and NH_4NO_3, respectively, and $f_{SS}(RH)$ is the water growth factor

for sea salt, which can be refer to Pitchford *et al.* (2007). Concentrations of $(NH_4)_2SO_4$, NH_4NO_3, and OM in the large and small mode are estimated by the following empirical equations (by taken $(NH_4)_2SO_4$ as an example):

$$[\text{Large (NH}_4)_2\text{SO}_4] = [\text{Total (NH}_4)_2\text{SO}_4]^2/20,$$
$$\text{for } [\text{Total (NH}_4)_2\text{SO}_4] < 20 \; \mu g \; m^{-3} \tag{14}$$

$$[\text{Large (NH}_4)_2\text{SO}_4] = [\text{Total (NH}_4)_2\text{SO}_4],$$
$$\text{for } [\text{Total (NH}_4)_2\text{SO}_4] \geq 20 \; \mu g \; m^{-3} \tag{15}$$

$$[\text{Small (NH}_4)_2\text{SO}_4] =$$
$$[\text{Total (NH}_4)_2\text{SO}_4] - [\text{Large (NH}_4)_2\text{SO}_4] \tag{16}$$

where total mass concentrations of $(NH_4)_2SO_4$, NH_4NO_3, OM, FS, and sea salt are estimated by the same methods as those described in Section of "*Reconstruction of PM$_{2.5}$ Mass*". The contribution of coarse mass to b_{ext} is negligible (Jung *et al.*, 2009) and excluded from the analysis due to no coarse mass data in this study. The units for b_{ext} and dry efficiency terms are in Mm^{-1} and $m^2 \, g^{-1}$, respectively; chemical composition concentrations are in $\mu g \; m^{-3}$, $f(RH)$ is dimensionless.

Original visual ranges (VRs) were obtained from the environmental monitoring station of Ya'an city. From June 2013 to November 2013, there were 8 synoptic observations per day started from 23:00. From December 2013 to June 2014, there were 24 synoptic observations per day started from 21:00. Considered that the PM$_{2.5}$ samples were collected from 10:00 to 10:00 next day, the final daily average VRs were recalculated according to the practical sampling schedule. In comparison, VRs were estimated from light extinction coefficient according to the Koschmieder equation (Koschmieder 1924):

$$VR = 3.912 \times 1000/b_{ext} \tag{17}$$

where b_{ext} is calculated from Eq.13, and the units of VR and b_{ext} are km and Mm^{-1}, respectively. In addition, the data of daily sulfur dioxide (SO$_2$), nitrogen dioxide (NO$_2$), wind speed (WS), temperature, RH, and rainfall were obtained from the Ya'an Meteorological Bureau, where located at 500 m northeast to the sampling site.

RESULTS AND DISCUSSION

Characteristics of Visibility

Fig. 5 shows the time series of VR, SO$_2$, NO$_2$, and meteorological parameters of this study. Those samples collected in summer, from June to August 2013 and June 2014, were integrated when seasonal variation was discussed. The daily average VR varied from 0.79 to 38.8 km during the whole sampling period, with an average of 11.9 ± 9.2 km. The highest average VR of 20.1 km was seen in summer, followed by autumn (15.0 km) and spring (8.3km). The lowest VR was seen in winter (4.0 km), while its VRs were all below 10 km (Fig. 5). On annual average, the VR in Ya'an was higher than those reported in Chinese megacities, including Beijing, Guangzhou, Shanghai, Chengdu, Xi'an,
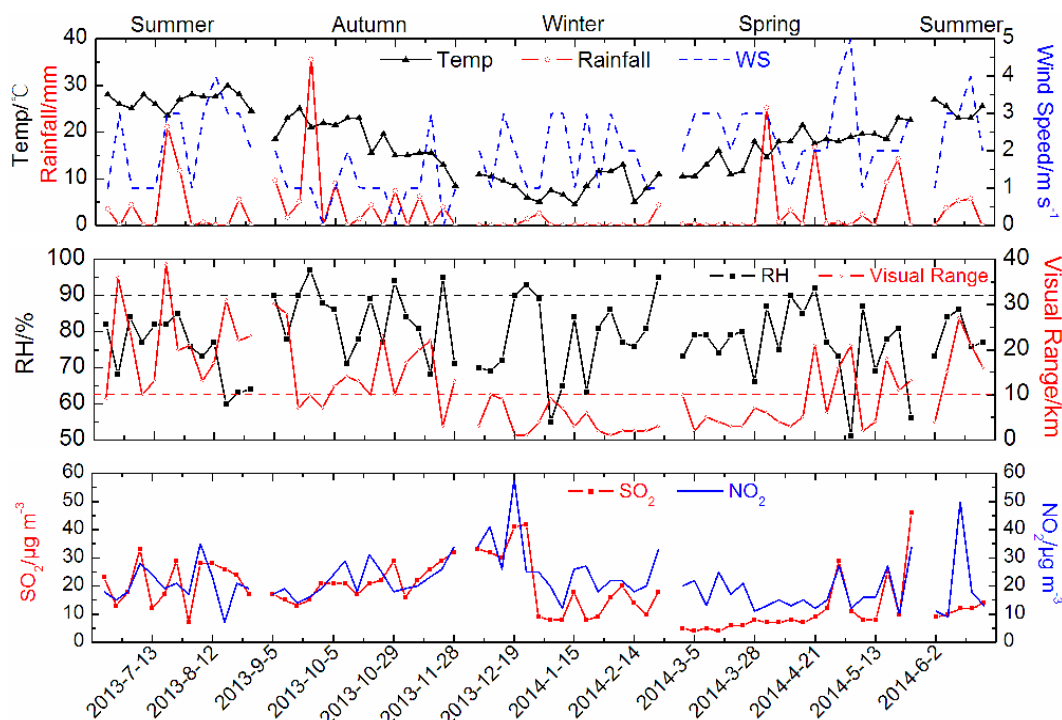
Fig. 5. Time series of visual range, SO_2, NO_2, and meteorological parameters on the sampling days. Black and red dash line present 90% RH and 10 km VR, respectively.

Shenyang, and urban areas of Taiwan and Kaohsiung (Cheng and Tsai, 2000; Chang *et al.*, 2009; Cao *et al.*, 2012; Wang *et al.*, 2013; Yuan *et al.*, 2006), but was lower than those reported from Xiamen, remote areas of Taiwan, and rural site of central Pearl River Delta region (Cheng and Tsai, 2000; Wang *et al.*, 2012; Zhang *et al.*, 2012).

VR was negatively correlated to $PM_{2.5}$ ($r = –0.57$) and its major components, especially OC and secondary inorganic ions including $SO_4^{2–}$, $NO_3^–$, and NH_4^+ with r in range of –0.52 to –0.72 (Table 1), that were consistent with previous studies (Cao *et al.*, 2012; Chen *et al.*, 2014). While VR was fairly correlated to temperature ($r = 0.57$) but had poor correlations with RH ($r = –0.22$), WS ($r = 0.25$), and rainfall ($r = 0.23$). As shown in Fig. 5, higher temperatures (26.3°C on average) and wind speed (2.3 m s^{-1} on average) were seen in summer, indicating that the greatest vertical mixing and favorable diffusion conditions among the four seasons, as a result of the lowest $PM_{2.5}$ mass levels. Even though poor correlation with VR was seen in this study, precipitation had great impacts on the $PM_{2.5}$ concentrations due to scavenging effect. The highest precipitation in summer, with a value of 961 mm (58% of the value measured in 2013), coincided with the lowest $PM_{2.5}$ concentration. Furthermore, 73% of sampling days with VR < 10 km were associated with no and/or less than 1.4 mm precipitation in this study. It is worth to noting that the rainfall values shown in Fig. 5 were only accounted for the sampling days. However, the precipitation value of 961 mm was the sum of values in summer. Any rain occurred before the sampling could have great influences on the $PM_{2.5}$ mass concentrations. This may vary the results of their correlation analysis. RHs were stable (on average, from 76.1% in summer to 83.5% in

autumn) in Ya'an which thus had insignificant contribution to the seasonal variations of VR. Such observation was different from Beijing, where the lowest VR was found in summer due to high RHs, while the highest VR was seen in winter at higher wind speed and lower RH (Zhang *et al.*, 2010; Zhao *et al.*, 2011). Hence, more negative correlations between VR and RH were observed in Beijing ($r = –0.83$) (Chen *et al.*, 2014) and Xi'an ($r = –0.71$) (Cao *et al.*, 2012).

Deng *et al.* (2008) and Zhao *et al.* (2011) defined that any day with VR <10 km and RH < 90% is haze, whereas RH ≥ 90% is belong to fog. The total number of hazy days was 31 in this study which most frequently occurred in spring and winter. The percentage of haze to the total amount of samples was 44.3%, which was much higher than the study conducted in non-urban (11%) and urban (17%) in Beijing, Tianjing, and Hebei region (Zhao *et al.*, 2011). Similarly, the frequency of fog days in Ya'an (14.3%, 10 of 70 samples) was also higher than that study (< 2.5%) (Zhao *et al.*, 2011). And between, 60% of our fog days were with VR < 10 km. The median visibility has decreased from 22.9 km (average taken from 2001–2005) to 18 km (average taken from 2006–2010). The number of days with visibility >19 km also decreased from 130 between 2001–2005 to 124 between 2006–2010, while the number of days with visibility < 10 km increased from 70 between 2001–2005 to 80 between 2006–2010 (Chen and Xie, 2012). Our study further indicates that the median visibility in Ya'an rapidly decreased to 9.8 km in 2013/2014, and the numbers of days with visibility > 19 km significantly reduced to 70 and with visibility < 10 km even increased to 184. These observations obviously prove that the visibility deterioration has been accelerating in Ya'an since 2000s.

Table 1. Correlation coefficients of visibility with $PM_{2.5}$ and its major components, as well as meteorological parameters.

	$PM_{2.5}$	OC	EC	Cl^-	SO_4^{2-}	NO_3^-	Na^+	NH_4^+	K^+	Mg^{2+}	Ca^{2+}	Temp	RH	Rainfall	WS
r	**-0.57**	**-0.54**	-0.42	-0.34	**-0.52**	**-0.66**	-0.33	**-0.72**	-0.27	-0.06	0.35	**0.57**	-0.22	0.23	0.25

Correlations between $PM_{2.5}$ and Visual Range

Seven major chemical components were determined in this study, consistent with those applied in the revised IMPROVE method (Pitchford *et al.*, 2007), are dominant species in dry particles and successfully used to reconstruct the $PM_{2.5}$ mass (Hsu *et al.*, 2010; Tao *et al.*, 2014; Wang *et al.*, 2015a). Table 2 lists the levels of reconstructed $PM_{2.5}$ mass and its chemical components. The highest average $PM_{2.5}$ mass was seen in winter (104.6 ± 61.5 μg m^{-3}), followed by spring (63.4 ± 26.8 μg m^{-3}), autumn (52 ± 20.8 μg m^{-3}), and summer (39.7 ± 14 μg m^{-3}), that was opposite to the trend of visibility. The annual mean of $PM_{2.5}$ mass in Ya'an (64.1 ± 41.6 μg m^{-3}) were ~4 and ~2 times exceeded the National Ambient Air Quality Standards (NAAQS) in US (15 μg m^{-3}) and China (35 μg m^{-3}), respectively.

On the base of annual averages, the compositions of the major chemical components had a descending order of OM > $(NH_4)_2SO_4$ > NH_4NO_3 > water > FS > EC > K_{BB} > TEO > CS. OM was the most abundant component (10.8–39 μg m^{-3}), accounting for 27.8–40.2% (with an annual average of 32.8%) of $PM_{2.5}$ mass. The percentages of $(NH_4)_2SO_4$ (21.6–35.6%, annual 28.3%) were more than twice those of NH_4NO_3 (4.4–16.9%, annual 12.1%) in Ya'an, that was similar to observations in Chengdu (16.3%–33.2% and 9.7%–17.3% (Tao *et al.*, 2013); and 23.9%–35.5% and 7.4%–15.1% (Tao *et al.*, 2014), for $(NH_4)_2SO_4$ and NH_4NO_3, respectively), but different from the finding in Beijing (29.7% and 23.3% for $(NH_4)_2SO_4$ and NH_4NO_3, respectively) (Wang *et al.*, 2015b), where extraordinary of NH_4NO_3 was due to the highest contribution from vehicle emission (Chen *et al.*, 2014; Wang *et al.*, 2015b). FS contributed 6.5–13.7% of $PM_{2.5}$, that was also consistent to the case in Chengdu (4.1–12.4%) (Tao *et al.*, 2013). The contributions of EC in Ya'an (1.5–2.0%) were lower than those of Chengdu (4.5–6.3% (Tao *et al.*, 2013) and 5.2–6.2% (Tao *et al.*, 2014)) and Beijing (3.5–6.2%) (Wang *et al.*, 2015b). This can be ascribed to the relatively less number of vehicles in Ya'an than those of mega-provincial capitals, and more usage of natural gas as fuel for automobiles (e.g., taxis) due to its low cost. The annual contributions of CS, TEO, and K_{BB} to $PM_{2.5}$ were close which were in ranges of 0.7–1.1%. Owing to water content estimated at a fixed RH and temperature, its percentages showed little variation which accounted for 12% of $PM_{2.5}$, consistent to ~13% reported by Tao *et al.* (2014). However, if the water content was estimated at daily ambient RH and temperature, the annual concentration of water would significantly increase from 7.6 μg m^{-3} to 41.44 μg m^{-3} in Ya'an. Water would become the most abundant and evidently affects the extinction property of aerosol.

Observed VRs were exponentially associated with daily $PM_{2.5}$ mass ($r = 0.69$, Fig. 6(a)), consistent with the linear relationship between $PM_{2.5}$ and b_{ext}. The threshold $PM_{2.5}$ mass corresponding to VR = 10 km was ~59 μg m^{-3}. This value was ~21% lower than the guideline of 75 μg m^{-3} set by China NAAQS. There were 42.9% of total samples with $PM_{2.5}$ > 59 μg m^{-3}, which was consistent with our previous discussed, that is, 44.3% of total samples were collected in hazy days in this study. The low threshold value was mainly caused by high RHs in Ya'an. In Beijing, the RH mostly

Table 2. Seasonal and annual concentrations of $PM_{2.5}$ and its chemical components (µg m^{-3}), as well as meteorological parameters in Ya'an.

	Spring (n = 20)	Summer (n = 18)	Autumn (n = 16)	Winter (n = 16)	Annual (n = 70)
Reconstructed $PM_{2.5}$	63.4 ± 26.8	39.7 ± 14	52 ± 20.8	104.6 ± 61.5	64.1 ± 41.6
$(NH_4)_2SO_4$	17 ± 8.7	14.2 ± 6	14.4 ± 6.2	23.8 ± 16.8	17.3 ± 10.7
NH_4NO_3	10.5 ± 7.3	1.8 ± 1.7	6.7 ± 4.7	17 ± 9.1	8.9 ± 8.3
OM	19.6 ± 9	10.8 ± 4.1	17.5 ± 8.8	39 ± 17.7	21.3 ± 14.7
EC	1 ± 0.4	0.7 ± 0.2	0.9 ± 0.4	1.4 ± 0.5	1 ± 0.5
FS	5.9 ± 3.2	5.8 ± 4.3	4.7 ± 2.4	8.3 ± 12.4	6.1 ± 6.6
CS	0.4 ± 0.2	0.3 ± 0.1	0.4 ± 0.2	0.5 ± 0.2	0.4 ± 0.2
TEO	0.5 ± 0.1	0.6 ± 0.2	0.6 ± 0.2	0.7 ± 0.6	0.6 ± 0.3
K_{BB}	0.8 ± 0.9	0.3 ± 0.2	0.5 ± 0.2	2.2 ± 4.4	0.9 ± 2.3
Water	7.6 ± 3.8	5.3 ± 2.1	6.3 ± 2.5	11.7 ± 7.7	7.6 ± 5
TEMP/℃	16.9 ± 3.9	26.3 ± 2	18.4 ± 4.6	8.6 ± 2.7	17.8 ± 7.1
RH/%	76.6 ± 10.4	76.1 ± 7.9	83.6 ± 9	77.9 ± 11.6	78.3 ± 10
PR/mm*	306.7	961.1	329.3	68.8	1665.9
WS/m s^{-1}	2.39 ± 0.82	2.31 ± 1	1.09 ± 0.73	1.93 ± 0.97	1.97 ± 1.01
SO_2/µg m^{-3}	11.3 ± 10.4	18.4 ± 8	21.1 ± 5.6	20.2 ± 13.4	17.3 ± 10.2
NO_2/µg m^{-3}	17.7 ± 6.4	20.3 ± 9.9	22 ± 5.7	26.9 ± 11.9	21.2 ± 9
VR/km	8.3 ± 6.3	20.1 ± 9.2	15 ± 7.7	4 ± 3.1	11.9 ± 9.2
Reconstructed $PM_{2.5}$**	90.7 ± 42.0	51.6 ± 18.8	93.8 ± 39.5	163.2 ± 108.7	97.9 ± 71.1
Water **	34.9 ± 24	17.2 ± 9.1	48.1 ± 36.8	70.2 ± 63.6	41.4 ± 41.5

* Considering that rainfall before sampling days might have great influence on the mass concentration of $PM_{2.5}$, here the PR values are the sum of each season and the whole year, neither average ones nor only sum of the sampling day values.
** here both water and reconstructed $PM_{2.5}$ were calculated at ambient RH and temperature conditions.
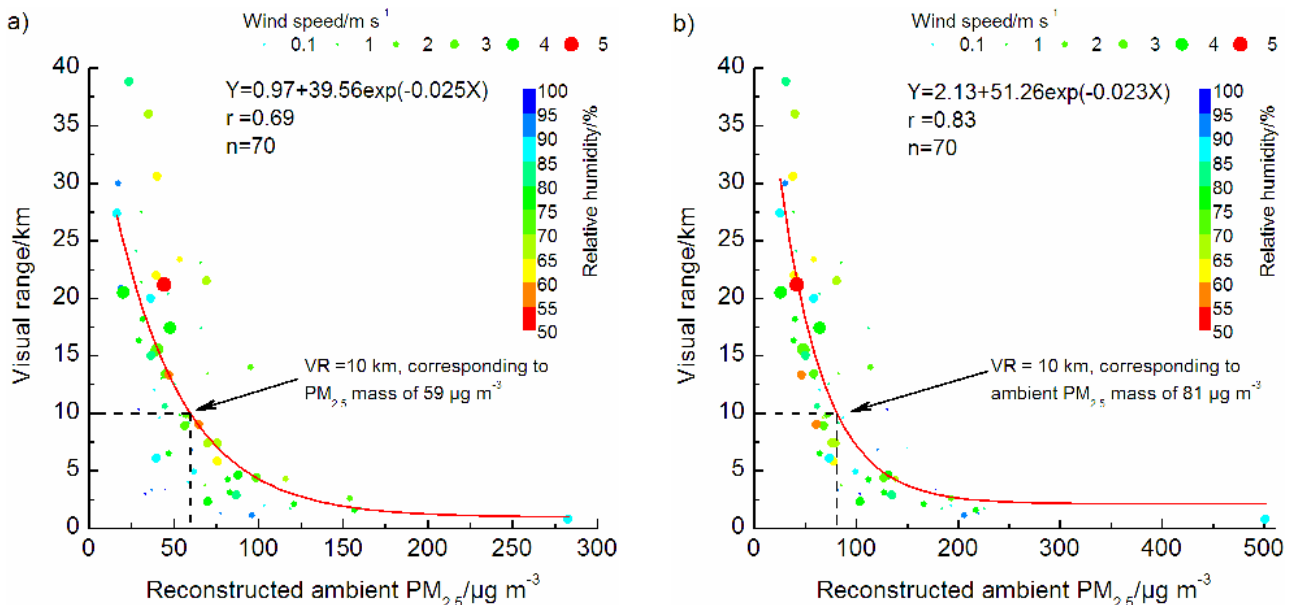

Fig. 6. Visual range as a function of $PM_{2.5}$ mass in Ya'an. a) on a base of water contents calculated at fixed RH (40%) and temperature (20°C), b) on a base of water contents calculated at ambient RH and temperature. Data points are color coded for RH and size coded for WS.

ranged from 20 to 40% for "good" hours with VR ≥ 20 km between the years of 1999 and 2007, and the lowest mean visibility was found in summer due to relatively higher RHs among the seasons (Zhang *et al.*, 2010). In comparison with Beijing, there are stiffer challenges in improvement of visibility in much humic atmospheres of Ya'an and Sichuan basin. If the water contents were estimated at ambient RH

and temperature, the reconstructed ambient $PM_{2.5}$ had a better correlation coefficient ($r = 0.83$, Fig. 6(b)) with VR, reflecting the strong impact of RHs on the concentration and optical property of $PM_{2.5}$ in ambient environments.

Fig. 7 compares the observed and calculated VR from Eq. (17). It is obviously that the calculated VRs had a good correlation with the observed ones ($r = 0.82$, slope = 0.94).
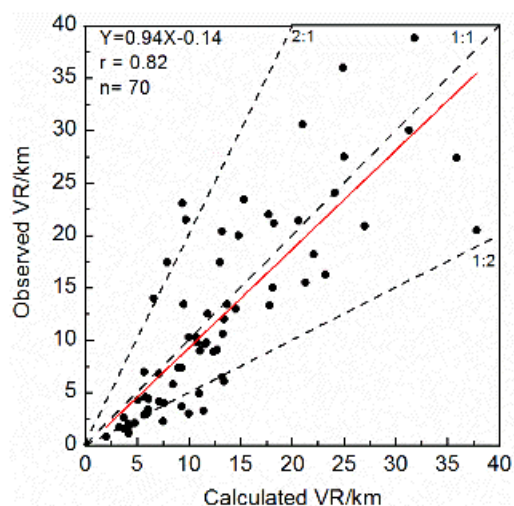
Fig. 7. Comparison of observed and calculated VR.

For the low observed VRs, almost all calculated values had positive deviations, indicating that the reconstructed b_{ext} could be under-estimated. For the high observed VRs, the calculated ones can be either over- or under-estimated. The ratios of observed to calculated values ranged from 0.5 to 2.0 in this study. Considering that the assumptions for Eq. (17) could not be perfectly implied in real ambient conditions and the potential errors in reconstruction b_{ext}, the deviations between observed and calculated VRs were reasonable.

Contributions of Chemical Component to Light Extinction

The seasonal variations of b_{ext} as well as the contribution of each component to b_{ext} are shown in Fig. 8. With Eq. (13), dry extinction coefficients ($b_{ext, dry}$) were estimated with f(RH) = 1, while ambient extinction coefficients ($b_{ext, RH}$) were estimated in which the hygroscopic growth of inorganic components was considered. As illustrated in Fig. 8, the

highest $b_{ext, RH}$ was seen in winter (769 ± 429 Mm^{-1}), followed by spring (436 ± 228 Mm^{-1}), autumn (403 ± 162 Mm^{-1}) and summer (231 ± 91 Mm^{-1}), with an annual value of 452 ± 314 Mm^{-1}. Compared with other Chinese cities, the annual b_{ext} in Ya'an was lower than that in Jinan (778 Mm^{-1} and 528 Mm^{-1} for urban and rural sites, respectively) (Yang *et al.*, 2012), Beijing (880 Mm^{-1}) (Wang *et al.*, 2015b), Chengdu (900 Mm^{-1}) (Wang *et al.*, 2013) and Xi'an (912 Mm^{-1}) (Cao *et al.*, 2012), but was higher than that in Guangzhou (367 Mm^{-1}) (Jung *et al.*, 2009) and Xiamen (214 Mm^{-1}) (Zhang *et al.*, 2012). However, the average annual reconstructed $b_{ext,dry}$ was only 268 ± 182 Mm^{-1}, indicating that ~40.8% of ambient $b_{ext, RH}$ was contributed by the factor of RH. The contribution of RH to $b_{ext, RH}$ of this study was higher than the finding in Wang *et al.* (2015b) due to higher RHs in Ya'an than Beijing. On annual average, 26.4% and 14.0% of the increasing were attributed to the water growth on (NH$_4$)$_2$SO$_4$ and NH$_4$NO$_3$, respectively, while only 0.4% was from CS. The highest contribution of RH to $b_{ext, RH}$ was found in autumn (47.1%), followed by winter (39.9%), spring (39.0%), and the summer (37.2%), consistent with the seasonal variation of RHs. The formations of secondary inorganic, especially (NH$_4$)$_2$SO$_4$ and NH$_4$NO$_3$, and organic compounds could be also enhanced under humid conditions through heterogeneous oxidations (Yu *et al.*, 2005; Hennigan *et al.*, 2008). Besides, the fine hydrophilic species could promote the water uptake of aerosols, which can enlarge in size and deteriorate visibility through enhanced light scattering (Malm *et al.*, 2013; Chen *et al.*, 2014). These mechanisms can be explained to the significant impacts of RH on VR.

As shown in Fig. 8, (NH$_4$)$_2$SO$_4$, OM and NH$_4$NO$_3$ are the three most dominant chemical components, totally accounting for 92.6% of the total $b_{ext,RH}$. (NH$_4$)$_2$SO$_4$ was the largest contributor, accounting for 43.1% of total $b_{ext,RH}$, followed by OM (27.1%), NH$_4$NO$_3$ (22.4%), while Rayleigh (2.43%), EC (2.27%), fine soil (1.36%), NO$_2$ (0.79%), and chloride salt (0.57%) had much minor contributions. It should be noted that
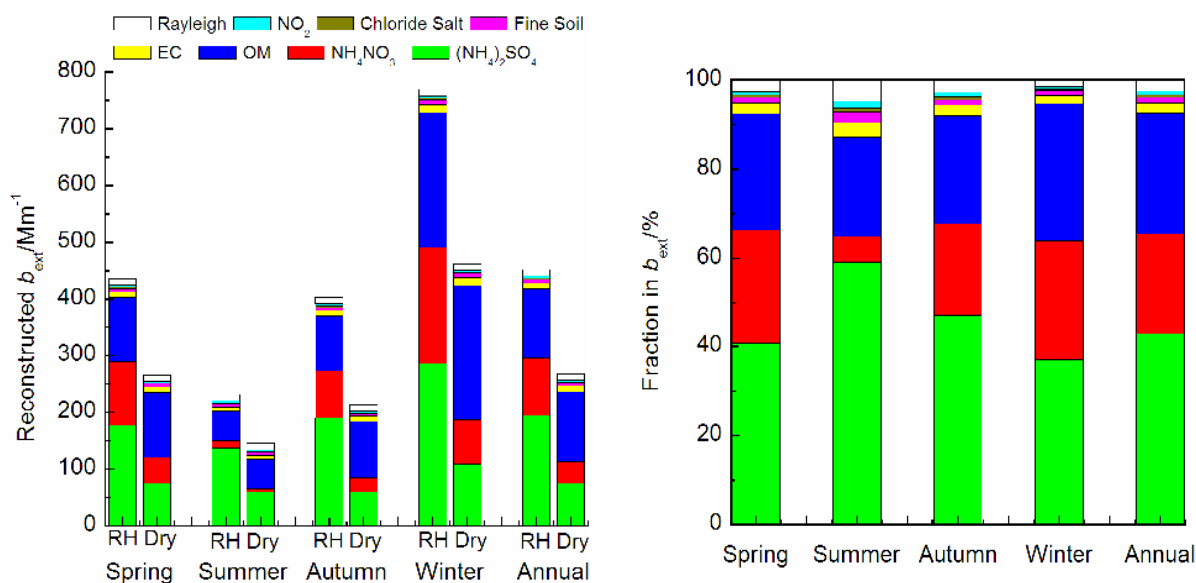

Fig. 8. Seasonal variations of b_{ext} and contributions of each species to the total $b_{ext,RH}$.

there was an evident seasonal variation on the contributions to $b_{ext,RH}$ from each component. The contributions of $(NH_4)_2SO_4$ to $b_{ext,RH}$ in summer (59.1%) and autumn (47.2%) were higher than the annual average of 43.1%, while much lower seasonal contributions were seen in spring (40.7%) and winter (37.1%). The result indicates that high temperature and strong solar radiation facilitate the formation of secondary inorganic species. In contrast, the contribution of NH_4NO_3 was the lowest in summer, accounting only for 5.8% of total $b_{ext,RH}$, in comparison of 20.5–26.8% reported in other seasons, the most important reason is that particulate NH_4NO_3 was prone to decompose and redistribute in gas-phase under high temperature in summer. Moreover, the contribution of OM elevated in winter (30.8%), while no significant variation was found in other seasons (22.3–26.1%).

We compared the chemical b_{ext} under good and poor visibility by classifying 10% of the days with the best visibility (VR > 24 km, n = 7, abbreviated as Best 10%) and 10% of the days with the worst visibility (VR < 2 km, n = 7, abbreviated as Worst 10%) (Table 3). Among the Worst 10%, six of the days were in winter while one was in spring. The day with poor visibility in winter can be ascribed to the letting-off firework within the period of Spring Festival, additionally combined with low temperature and low precipitation (Fig. 2) that facilitated a low mixing height and inversion layer and thus caused pollutant accumulation. Severe haze during the Spring Festival were often reported (e.g., Feng *et al.*, 2012; Kong *et al.*, 2015). The day with poor visibility on May 9, 2014 coincided with ploughing and biomass burning occurred in spring, conformed by its relatively high concentration of K_{BB} (2.59 μg m^{-3}). Smoke emitted from biomass burning is mainly in the form of sub-micrometer and accumulation mode, which could increase the rates of chemical reactions for secondary aerosol formation under high RHs (Balasubramanian *et al.*, 1999; Yao *et al.*, 2016). Among the Best 10%, five were in summer and two were in early autumn. Strong scavenging effect of pollutants by abundant precipitation and the decomposition of NH_4NO_3 under high temperatures were the reasonable explanations for the good visibility.

For the Worst 10%, $(NH_4)_2SO_4$ (42.6%) was the largest b_{ext} contributor, followed by NH_4NO_3 (26.8%) and OM (26.2%). The three dominated contributors accounted for 95.6% of b_{ext}, consistent with those reported in Xi'an (Cao *et al.*, 2012) and Beijing (Wang *et al.*, 2015b). For the Best 10%, $(NH_4)_2SO_4$ (48.9%) and OM (25.0%) were more significant contributors, accounting for 73.9% of b_{ext}. Our observation was different from the findings in Xi'an and Beijing, where OM had higher contributions than $(NH_4)_2SO_4$ under good visibility. The average contributions of $(NH_4)_2SO_4$, NH_4NO_3 and OM to the b_{ext} in the Worst 10% were 481.8, 303.3 and 296.5 Mm^{-1}, respectively, which were 6.8, 31.4 and 8.1 times higher than those for the Best 10%. The most significant difference between the Best 10% and the Worst 10% was the contribution of NH_4NO_3 (6.6% vs. 26.8%) due to its volatility and instability. As discussed above, centralized human activities, such as firework in the Spring Festival and biomass burning activities in ploughing period in spring, must be controlled to prevent the pollution episodes. It is also worth noting that $(NH_4)_2SO_4$, NH_4NO_3 and OM were responsible for the visibility deterioration in Ya'an. Reductions of their precursors such as SO_2, NO_x, NH_3 and volatile organic compounds by restrict emission control measures could effectively improve the visibility in Ya'an.

CONCLUSIONS

The chemical composition of $PM_{2.5}$ in Ya'an, Sichuan Basin, which included OC, EC, water-soluble ions, and elements, was determined. The highest VR was found in summer, followed by autumn, spring, and winter. VRs were exponentially correlated with $PM_{2.5}$ mass ($r = 0.69$), and the $PM_{2.5}$ threshold value associated with VR = 10 km was ~59 μg m^{-3}. The high frequency of hazy days (44.3%), in addition to the rapid decrease in median VR to 9.8 km and the increase in the number of days with VR < 10 km since the 2000s, illustrates that the visibility deterioration has became more severe in Ya'an.

The annual average $PM_{2.5}$ concentration was 64.1 ± 41.6 μg m^{-3}. The OM, $(NH_4)_2SO_4$, and NH_4NO_3 were the top three components of $PM_{2.5}$. According to calculations using the revised IMPROVE equation, the estimated annual mean ambient b_{ext} was 452 ± 314 Mm^{-1}, with the highest value seen in winter, followed by spring, autumn, and summer. For the annual average, $(NH_4)_2SO_4$ had the largest contribution, at 43.1%, to b_{ext}, followed by OM (27.1%) and NH_4NO_3 (22.4%). Low threshold $PM_{2.5}$ mass and the high contribution of RH to $b_{ext,RH}$ suggest that RH had a significant effect on the visibility impairment in Ya'an. Considering the characteristic culture in China, some centralized human

Table 3. Comparison of the contributions of major components to $b_{ext,RH}$ between the Best 10% and Worst 10% of observed VR.

	Best 10% (> 24 km, n = 7)		Worst 10% (< 2 km, n = 7)	
	Avg. ± SD (Mm^{-1})	% of $b_{ext,RH}$	Avg. ± SD (Mm^{-1})	% of $b_{ext,RH}$
$(NH_4)_2SO_4$	71.1 ± 13.5	48.9	481.8 ± 196.4	42.6
NH_4NO_3	9.6 ± 6.9	6.6	303.3 ± 79.4	26.8
OM	36.4 ± 21.1	25.0	296.5 ± 132.2	26.2
EC	7.3 ± 1	5.0	17.7 ± 4.9	1.6
FS	4.9 ± 2.3	3.3	12.9 ± 18	1.1
Chloride salt	1.6 ± 0.7	1.1	4.4 ± 1.3	0.4
NO_2	3.6 ± 2.4	2.5	3.4 ± 3.4	0.3
Rayleigh	11 ± 0	7.6	11 ± 0	1

activities must be regulated to prevent pollution episodes. More particularly, the discharge of precursors for poor visibility should be effectively reduced to improve the air quality and atmospheric visibility in the area.

ACKNOWLEDGMENTS

SUPPLEMENTARY MATERIAL

Supplementary data associated with this article can be found in the online version at http://www.aaqr.org.

REFERENCES

Bi, X., Feng, Y., Wu, J., Wang, Y. and Zhu, T. (2007). Source apportionment of PM_{10} in six cities of northern China. *Atmos. Environ.* 41: 903–912.

Birch, M. and Cary, R. (1996). Elemental carbon-based method for monitoring occupational exposures to particulate diesel exhaust. *Aerosol Sci. Technol.* 25: 221–241.

Brook, J.R., Dann, T.F. and Burnett, R.T. (1997). The relationship among TSP, PM_{10}, $PM_{2.5}$ and inorganic constituents of atmospheric particulate matter at multiple Canadian locations. *J. Air Waste Manage. Assoc.* 47: 2–19.

Cao, J.J., Wang, Q.Y., Chow, J.C., Watson, J.G., Tie, X.X., Shen, Z.X., Wang, P. and An, Z.S. (2012). Impacts of aerosol compositions on visibility impairment in Xi'an, China. *Atmos. Environ.* 59: 559–566.

Chang, D., Song, Y. and Liu, B. (2009). Visibility trends in six megacities in China 1973-2007. *Atmos. Res.* 94: 161–167.

Che, H., Zhang, X., Li, Y., Zhou, Z., Qu, J.J. and Hao, X. (2009). Haze trends over the capital cities of 31 provinces in China, 1981-2005. *Theor. Appl. Climatol.* 97: 235–242.

Chen, J., Qiu, S., Shang, J., Wilfrid, O.M.F., Liu, X., Tian, H. and Boman, J. (2014). Impact of relative humidity and water soluble constituents of $PM_{2.5}$ on visibility impairment in Beijing, China. *Aerosol Air Qual. Res.* 14: 260–268.

Chen, L.X., Zhang, B., Zhu, W.Q., Zhou, X.J., Luo, Y.F., Zhou, Z.J. and He, J.H. (2009). Variation of atmospheric aerosol optical depth and its relationship with climate change in China east of 100°E over the last 50 years. *Theor. Appl. Climatol.* 96: 191–199.

Chen, X. and Yu, J.Z. (2007). Measurement of organic mass to organic carbon ratio in ambient aerosol samples using a gravimetric technique in combination with chemical analysis. *Atmos. Environ.* 41: 8857–8864.

Chen, Y. and Xie, S. (2012). Temporal and spatial visibility trends in the Sichuan Basin, China, 1973 to 2010. *Atmos. Res.* 112: 25–34.

Cheng, M.T. and Tsai, Y.I. (2000). Characterization of visibility and atmospheric aerosols in urban, suburban, and remote areas. *Sci. Total Environ.* 263: 101–114.

Cheng, Z., Wang, S., Jiang, J., Fu, Q., Chen, C., Xu, B., Yu, J., Fu, X. and Hao, J. (2013). Long-term trend of haze pollution and impact of particulate matter in the Yangtze River Delta, China. *Environ. Pollut.* 182: 101–110.

Deng, X.J., Tie, X.X., Wu, D., Zhou, X.J., Bi, X.Y., Tan, H.B., Li, F. and Jiang, C.L. (2008). Long-term trend of visibility and its characterizations in the Pearl River Delta (PRD) region, China. *Atmos. Environ.* 42: 1424–1435.

Fountoukis, C. and Nenes, A. (2007). ISORROPIA II: A computationally efficient thermodynamic equilibrium model for K^+-Ca^{2+}-Mg^{2+}-NH_4^+-Na^+-SO_4^{2-}-NO_3^--Cl^--H_2O aerosols. *Atmos. Chem. Phys.* 7: 4639–4659.

Henriksson, S.V., Laaksonen, A., Kerminen, V.M., Raisanen, P., Jarvinen, H., Sundstrom, A.M. and de Leeuw, G. (2011). Spatial distributions and seasonal cycles of aerosols in India and China seen in global climate-aerosol model. *Atmos. Chem. Phys.* 11: 7975–7990.

Ho, K.F., Lee, S.C., Chan, C.K., Yu, J.C., Chow, J.C. and Yao, X.H. (2003). Characterization of chemical species in $PM_{2.5}$ and PM_{10} aerosols in Hong Kong. *Atmos. Environ.* 37: 31–39.

Hsu, S.C., Liu, S.C., Huang, Y.T., Lung, S.C.C., Tsai, F., Tu, J.Y. and Kao, S.J. (2008). A criterion for identifying Asian dust events based on Al concentration data collected from northern Taiwan between 2002 and early 2007. *J. Geophys. Res.* 113: 1044–1044.

Hsu, S.C., Liu, S.C., Tsai, F., Engling, G., Lin, I.I., Chou, C.K.C., Kao, S.J., Lung, S.C.C., Chan, C.Y., Lin, S.C., Huang, J.C., Chi, K.H., Chen, W.N., Lin, F.J., Huang, C.H., Kuo, C.L., Wu, T.C. and Huang, Y.T. (2010). High wintertime particulate matter pollution over an offshore island (Kinmen) off southeastern China: An overview. *J. Geophys. Res.* 115: 1383–1392.

Jung, J., Lee, H., Kim, Y.J., Liu, X., Zhang, Y., Hu, M. and Sugimoto, N. (2009). Optical properties of atmospheric aerosols obtained by in situ and remote measurements during 2006 Campaign of Air Quality Research in Beijing (CAREBeijing-2006). *J. Geophys. Res.* 114: 1065–1066.

Koschmieder, H. (1924). Theorie der horizontalen Sichtweite. *Beitr. Phys. freien Atmos.* 12: 33–53.

Landis, M.S., Norris, G.A., Williams, R.W. and Weinstein, J.P. (2001). Personal exposures to $PM_{2.5}$ mass and trace elements in Baltimore, MD, USA. *Atmos. Environ.* 35: 6511–6524.

Li, X., He, K., Li, C., Yang, F., Zhao, Q., Ma, Y., Cheng, Y., Ouyang, W. and Chen, G. (2013). $PM_{2.5}$ mass, chemical composition, and light extinction before and during the 2008 Beijing Olympics. *J. Geophys. Res.* 118: 12158–12167.

Malm, W., Day, D.E., Kreidenweis, S.M., Collett, J.L. and Lee, T. (2003). Humidity-dependent optical properties of fine particles during the Big Bend Regional Aerosol and Visibility Observational Study. *J. Geophys. Res.* 1089: 469–474.

Malm, W.C., Sisler, J.F., Huffman, D., Eldred, R.A. and Cahill, T.A. (1994). Spatial and seasonal trends in particle concentration and optical extinction in the United States. *J. Geophys. Res.* 99: 1347–1370.

Pitchford, M., Malm, W., Schichtel, B., Kumar, N., Lowenthal, D. and Hand, J. (2007). Revised algorithm for estimating light extinction from improve particle speciation data. *J. Air Waste Manage. Assoc.* 57: 1326–1336.

Swami, K., Judd, C.D., Orsini, J., Yang, K.X. and Husain, L. (2001). Microwave assisted digestion of atmospheric aerosol samples followed by inductively coupled plasma mass spectrometry determination of trace elements. *Anal. Bioanal. Chem.* 369: 63–70.

Tao, J., Cheng, T.T., Zhang, R.J., Cao, J.J., Zhu, L.H., Wang, Q.Y., Luo, L. and Zhang, L.M. (2013). Chemical composition of PM$_{2.5}$ at an urban site of Chengdu in southwestern China. *Adv. Atmos. Sci.* 30: 1070–1084.

Tao, J., Zhang, L., Cao, J., Hsu, S.C., Xia, X., Zhang, Z., Lin, Z., Cheng, T. and Zhang, R. (2014). Characterization and source apportionment of aerosol light extinction in Chengdu, southwest China. *Atmos. Environ.* 95: 552–562.

Taylor, S.R. (1964). Abundance of chemical elements in the continental crust: A new table. *Geochim. Cosmochim. Acta* 28: 1273–1285.

Turpin, B.J. and Lim, H.J. (2001). Species contribution to PM$_{2.5}$ concentration: Revising common assumptions for estimating organic mass. *Aerosol Sci. Technol.* 35: 602–610.

Wang, H., Li, X., Shi, G., Cao, J., Li, C., Yang, F., Ma, Y. and He, K. (2015a). PM$_{2.5}$ chemical compositions and aerosol optical properties in Beijing during the late fall. *Atmosphere* 6: 164–182.

Wang, H., Tian, M., Li, X.H., Chang, Q., Cao, J., Yang, F., Ma, Y. and He, K. (2015b). Chemical composition and light extinction contribution of PM$_{2.5}$ in urban Beijing for a 1-year period. *Aerosol Air Qual. Res.* 15: 2200–2211.

Wang, H., Shi, G., Tian, M., Zhang, L., Chen, Y., Yang, F. and Cao, X. (2017). Aerosol optical properties and chemical composition apportionment in Sichuan Basin, China. *Sci. Total Environ.* 577: 245–257.

Wang, K., Dickinson, R.E. and Liang, S. (2009). Clear sky visibility has deceased over land globally from 1973 to 2007. *Science* 323: 1468–1470.

Wang, Q., Cao, J., Tao, J., Li, N., Su, X., Chen, L.W.A., Wang, P., Shen, Z., Liu, S. and Dai, W. (2013). Long-term trends in visibility and at Chengdu, China. *PLoS One* 8: e68894.

Wang, X.M., Ding, X., Fu, X.X., He, Q.F., Wang, S.Y., Bernard, F., Zhao, X.Y. and Wu, D. (2012). Aerosol scattering coefficients and major chemical compositions of fine particles observed at a rural site in the central Pearl River Delta, South China. *J. Environ. Sci.* 24: 72–77.

Watson, J.G. (2002). Visibility: Science and regulation. *J. Air Waste Manage. Assoc.* 52: 628–713.

Wu, C., Huang, X.H.H., Ng, W.M., Griffith, S.M. and Yu, J.Z. (2016). Inter-comparison of NIOSH and IMPROVE protocols for OC and EC determination: Implications for inter-protocol data conversion. *Atmos. Meas. Tech.* 9: 4547–4560.

Wu, J., Fu, C., Zhang, L. and Tang, J. (2012). Trends of visibility on sunny days in China in the recent 50 years. *Atmos. Environ.* 55: 339–346.

Yang, H., Yu, J.Z., Ho, S.S.H., Xu, J.H., Wu, W.S., Wan, C.H., Wang, X.D., Wang, X.R. and Wang, L.S. (2005). The chemical composition of inorganic and carbonaceous materials in PM$_{2.5}$ in Nanjing, China. *Atmos. Environ.* 39: 3735–3749.

Yu, J.Z., Xu, J. and Yang, H. (2002). Charring characteristics of atmospheric organic particulate matter in thermal analysis. *Environ. Sci. Technol.* 36: 754–761.

Yuan, C.S., Lee, C.G., Liu, S.H., Chang, J.C., Yuan, C. and Yang, H.Y. (2006). Correlation of atmospheric visibility with chemical composition of Kaohsiung aerosols. *Atmos. Res.* 82: 663–679.

Zhang, F.W., Xu, L.L., Chen, J.S., Yu, Y.K., Niu, Z.C. and Yin, L.Q. (2012). Chemical compositions and extinction coefficients of PM$_{2.5}$ in peri-urban of Xiamen, China, during June 2009-May 2010. *Atmos. Res.* 106: 150–158.

Zhang, Q.H., Zhang, J.P. and Xue, H.W. (2010). The challenge of improving visibility in Beijing. *Atmos. Chem. Phys.* 10: 7821–7827.

Zhang, X.Y., Wang, Y.Q., Niu, T., Zhang, X.C., Gong, S.L., Zhang, Y.M. and Sun, J.Y. (2012). Atmospheric aerosol compositions in China: Spatial/temporal variability, chemical signature, regional haze distribution and comparisons with global aerosols. *Atmos. Chem. Phys.* 12: 779–799.

Zhao, P., Zhang, X., Xu, X. and Zhao, X. (2011). Long-term visibility trends and characteristics in the region of Beijing, Tianjin, and Hebei, China. *Atmos. Res.* 101: 711–718.